Title

Intestinal bacterial indicator phylotypes associate with impaired DNA double-stranded break sensors but augmented skeletal bone micro-structure.

Journal

Carcinogenesis, 41(4)

ISSN

0143-3334

Authors

Maier, Irene
Liu, Jared
Ruegger, Paul M
et al.

Publication Date

2020-06-17

DOI

10.1093/carcin/bgz204

Peer reviewed

Carcinogenesis, 2020, Vol. 41, No. 4, 483–489

doi:10.1093/carcin/bgz204
Advance Access Publication December 16, 2019
Original Article

ORIGINAL ARTICLE

Intestinal bacterial indicator phylotypes associate with impaired DNA double-stranded break sensors but augmented skeletal bone micro-structure

Irene Maier[1,*], Jared Liu[1], Paul M.Ruegger[2], Julia Deutschmann[3], Janina M.Patsch[4], Thomas H.Helbich[4], James Borneman[2] and Robert H.Schiestl[1,5]

[1]Department of Environmental Health Sciences, Fielding School of Public Health, University of California, Los Angeles 650 Charles E. Young Dr. South, Los Angeles, CA 90095, USA, [2]Department of Microbiology and Plant Pathology, University of California, Riverside, CA 92521, USA, [3]Department for Radiologic Technology, University of Applied Sciences Wiener Neustadt for Business and Engineering Ltd., Lower Austria, Austria, [4]Department of Biomedical Imaging and Image-Guided Therapy, Medical University of Vienna, Währinger Gürtel 18–20, A-1090 Vienna, Austria and [5]Department of Pathology, University of California, Los Angeles 650 Charles E. Young Dr. South, Los Angeles, CA 90095, USA

*To whom correspondence should be addressed. Tel: +001 310-267-2087; Fax: +001 310-267-2578; Email: irene.maier@meduniwien.ac.at
Correspondence may also be addressed to Robert H.Schiestl. Tel: +001 310-267-2087; Fax: +001 310-267-2578

Abstract

Intestinal microbiota are considered a sensor for molecular pathways, which orchestrate energy balance, immune responses, and cell regeneration. We previously reported that microbiota restriction promoted higher levels of systemic radiation-induced genotoxicity, proliferative lymphocyte activation, and apoptotic polarization of metabolic pathways. Restricted intestinal microbiota (RM) that harbors increased abundance of *Lactobacillus johnsonii* (LBJ) has been investigated for bacterial communities that correlated radiation-induced genotoxicity. Indicator phylotypes were more abundant in RM mice and increased in prevalence after whole body irradiation in conventional microbiota (CM) mice, while none of the same ten most abundant phylotypes were different in abundance between CM mice before and after heavy ion irradiation. *Muribaculum intestinale* was detected highest in female small intestines in RM mice, which were lacking *Ureaplasma felinum* compared with males, and thus these bacteria could be contributing to the differential amounts of radiation-induced systemic genotoxicity between the CM and RM groups. *Helicobacter rodentium* and *M.intestinale* were found in colons in the radiation-resistant CM phenotype. While the expression of interferon-γ was elevated in the small intestine, and lower in blood in CM mice, high-linear energy transfer radiation reduced transforming growth factor-β with peripheral interleukin (IL)-17 in RM mice, particularly in females. We found that female RM mice showed improved micro-architectural bone structure and anti-inflammatory radiation response compared with CM mice at a delayed phase 6 weeks postexposure to particle radiation. However, microbiota restriction reduced inflammatory markers of tumor necrosis factor in marrow, when IL-17 was reduced by intraperitoneal injection of IL-17 neutralizing antibody.

Introduction

The gut microbiota have been found to play a role in determining an individual's intrinsic susceptibility to cancer (1). Besides studies of known oncogenic pathogens such as *Helicobacter pylori* (2) in the development of gastric cancer, it has been reported that gut microbial disturbances during colitis can initiate colorectal cancer (3). We further studied microbiota-associated disturbances and systemic genotoxicity in a mouse model deficient of DNA damage sensor protein ataxia telangiectasia-mutated

Received: June 22, 2019; **Revised:** December 7, 2019; **Accepted:** December 13, 2019

Abbreviations

Atm	ataxia telangiectasia-mutated;
BIPs	bacterial indicator phylotypes;
CFU	colony-forming units;
CM	conventional microbiota;
DCs	dendritic cells;
DSBs	double-stranded DNA breaks;
DTT	dithiothreitol;
GERD	gastroesophageal reflux disease;
HZE	high-charge and energy;
IFN	interferon;
IL	interleukin;
LBJ	*Lactobacillus johnsonii*;
LET	linear energy transfer;
OTUs	operational taxonomic units;
RM	Restricted microbiota;
SI	small intestine;
TNF	tumor necrosis factor

(Atm). *Lactobacillus johnsonii* (LBJ) has been identified in pathogen-free restricted gut microbiota in these DNA repair deficient mice as the most prominent bacterium in mucosa cells of colon and small intestine (SI), and to reduce inflammation (4). Fewer studies, however, have examined whether the gut microbiota can modulate the effects of exogenous carcinogenic factors, such as exposure to ionizing radiation.

Ionizing radiation inflicts both a physiological insult by inducing direct damage to cells and tissues as well as oncogenic risk to surviving cells that have sustained DNA alterations. In particular, the exposure to high—linear energy transfer (LET) radiation resulted in delayed cell cycle progression (5). Prolonged expression of DNA damage marker γ-H2AX (6) and radiation-sensitive biomarkers of genetic instability have demonstrated being relevant to cellular injury (6,7), whereas other studies postulated intestinal radiation tolerance in high-fractionated proton radiotherapy (8). In this course interleukin (IL)-12 has been reported to convert Foxp3$^+$ Treg cells to interferon (IFN)-γ-producing Foxp3$^+$ T cells in response to microbial products in other than the murine intestinal organ and to inhibit colitis (9). This cytokine was found to protect mice from the lethal hematopoietic syndrome (10). The expression of pro-osteoclastogenic tumor necrosis factor (TNF) genes, however, was interrogated and reported to be enhanced by radiation-induced genotoxicity (11).

We recently reported that microbiota restriction promoted higher levels of genotoxicity and proliferative lymphocyte activation (12). Investigations of intestinal microbiota compositions, probiotics intervention, and longitudinal investigations of intraluminal conditions prior and post radiation exposure have not been available yet. High-LET radiation was employed to explore the synergistic effects of irradiation (IR)-induced intestinal microbiota changes and IL-17 neutralization on pro-osteoclastogenic bone loss. At last, the abundance of bacterial indicator phylotypes (BIPs) was studied to modulate microbiota compositions as a model for clinical traits in radiation therapy (13). Whereas the microbiome is revealing the pathological interaction of bacterial microbes with innate and cell-mediated immunity, genotoxicity is focused to correlate microbiota-associated phenotypes with the development of chronic human diseases (14).

Materials and methods

Radiation experiment

C57BL/6J pink-eyed unstable (wild-type p$^{un+/+}$) mice and *Atm*$^{+/+}$ mice, both from Jackson Laboratory (Bar Harbor, ME), were used bearing restricted microbiota (RM) and conventional microbiota (CM), respectively. RM mice were created from a colony that was originally re-derived by Caesarian section and inoculated with only a few bacterial species as previously described in [(15); see Supplementary information]. CM mice were treated with antibiotics followed by orogastric gavage of CM feces (4). CM and RM mice were shipped from the University of California, Los Angeles to the Brookhaven National Laboratory (Upton, NY) and exposed to protons (^{1}H) at 2.0 GeV/n, or silicon ions (^{28}Si) at 850 MeV/u as provided by the NASA Space Radiation Laboratory (NSRL). The total dose for each whole body IR was 100–150 cGy delivered homogenously over 4–10 min (with a dose rate of 40 cGy/min for ^{28}Si; 12–15 cGy/min for ^{1}H), while six animals at a time were restrained in conical plastic holders. In accordance with the Animal Research Committee and institutional guidelines at the University of California, Los Angeles (UCLA), C57 BL/6J p^{un} female CM and RM mice (six animals per groups of 10–12 week-old mice) were injected neutralizing anti-IL-17 antibody intraperitoneally (20 μg monoclonal rat IgG2A Clone #50104/100 μL; R&D Systems, Minneapolis, MN) and irradiated on site at NSRL. ELISA was performed on blood from these mice to measure IL-17 and transforming growth factor (TGF)-β at 3 weeks post-IR. Oral administration of LBJ was 10^9 colony-forming units (CFU) in 50 μL PBS before and at two days post-IR with ^{1}H.

Genotoxicity assays

Micronuclei were examined in blood normochromatic erythroblasts collected from LBJ-inoculated, anti-IL-17 treated, and high-LET treated mice at 6 h post-IR and stained with Wright–Giemsa (Sigma–Aldrich, St. Louis, MO). At least 1000 erythrocytes were counted at 100× magnification. Lymphocytes from 50 μL peripheral blood were collected by centrifugation before performing the γ-H2AX immunofluorescence assay at 4 weeks post-IR as described earlier (12).

Micro-computed tomography

Dissected right tibiae (time-point 6 weeks post-IR) from anti-IL-17 modulated and irradiated CM and RM mice were imaged by micro-computed tomography (micro-CT) 35 (SCANCO Medical AG, Brüttisellen, Switzerland) to *ex vivo* quantify trabecular bone microarchitecture by a direct 3D approach (16). Scan resolution was 6 μm isotropic voxel size. Using the growth plate as a reference, the scan region spanned distal 0.9 mm (150 × 0.006) of the semiautonomously defined trabecular region of interest adjacent to the endocortical boundary (17).

Illumina sequence analyses of intestinal bacteria

Intestinal mucosa-associated cells from CM and RM mice were isolated from either, jejunum and ileum (together SI), or mid colon using dithiothreitol (DTT) (18). The procedure enriches for lamina propria cells. Illumina bacterial 16S rRNA gene libraries were constructed, sequenced and processed into operational taxonomic units (OTUs) using methods similar to those described in (19). Bacterial OTUs were analyzed using edgeR and Pearson correlation using cor.test, which is a part of R-base, in R (R Core Team 2017).

Quantitative real-time-PCR

RNA was isolated from 50 μL blood using the QIAmp RNA Blood Minikit (Qiagen, Hilden, Germany) mainly one day post-IR of CM and RM mice. Bone marrow was collected 5 weeks post-IR by flushing femurs with 2 mL DMEM media. CD4$^+$ cells were collected from bone marrow with anti-CD4 magnetic microbeads (Miltenyi Biotec Inc., Auburn, CA) in a final volume of 400 mL. Quantitative RT-PCR was performed in duplicate per sample on an ABI 7500 Fast RT-PCR thermocycler using Taqman gene expression assays (Thermo) for *Nfkb1*, *Tgfb1*, and *Ifng*, and Fast SYBR Green Master Mix for *Il17a*, *Angptl4 (Fiaf)*, *Tnf*, *Il2*, *Ifng*, and *Ccl20* (details given in Supplementary information).

Results

Radiation-induced systemic genotoxicity is strongly influenced by gut microbiota

Young adult mice harboring two distinct gut microbiota—CM and RM—exhibited considerably different levels of systemic

genotoxicity at 28 days after high-LET radiation. When irradiated with 1.5 Gy high-energy protons (^{1}H, 2 GeV), RM mice showed significantly higher double-stranded DNA breaks (DSBs) than CM mice (Figure 1A, $P < 0.0001$ for CM-IR vs. RM-IR. In fact, IR did not increase the formation of γ-H2AX foci in CM mice compared to non-irradiated (control) CM mice, but there was a greater than 10-fold increase in DNA damage in RM mice after 4 weeks post-IR (Figure 1). Chromosomal damage was measured by the alkaline comet assay in leukocytes of female mice at 6 h post-IR with either high-energy and -LET ^{1}H, or high-LET ^{28}Si ions (12). At both acute and delayed time-points, RM mice showed more single- and double-stranded DNA breaks than CM mice regardless of the type of radiation particles. In addition, the susceptibility of RM mice to high-LET-induced systemic genotoxicity and persistent DNA damage was associated with lower numbers of gut bacteria species prior to IR, as estimated by Chao1 analyses (Figure 1B, $P = 0.0013$ for CM > RM). To examine the relationship of specific bacteria taxa and radiation-induced genotoxicity, we analyzed translocating bacteria and bacterial compositions in lamina propria cells in the specified treatment and microbiota groups. Genotype- and age-matched CM and RM mice harbored several differentially abundant taxa.

Compared to SI with fewer variations, in the colon eight of these ten largest OTUs had different relative abundances between CM and RM mice (Table 1 and Supplementary Table 2A, $P < 0.05$, FDR-corrected). Five of the eight were greater in CM (*Helicobacter, Bacteroides*, and *Lactobacillus*) than RM mice while three were greater in RM mice (*Hymenobacteraceae*). Corroborating this assertion, most (6/8) of the bacterial OTUs that were differentially abundant in CM and RM mice before IR, were also differentially abundant post-IR. *Helicobacter, H.typhlonius*, and *H.rodentium*, as well as *Bacteroides stercoris* in this study, and carcinogenesis-related *Helicobacter hepaticus* (20) were strongly associated with the radiation-resistant phenotype as exhibited by the CM mice (12). Finally, six OTUs correlated with rather low genotoxicity (*Helicobacter, Mucispirillum, Clostridium_XVIII; Ruminococcaceae* and *Porphyromonadaceae* at the classification Family level, and Firmicutes *Clostridia*—Supplementary Table 2) in irradiated male mice. Our analyses separately examined animals by sex and age, and after treatment with the probiotic *Lactobacillus j. 456* (LBJ). An unclassified Gram-negative species cTPY-13 and LBJ were more abundant in RM mice, and inversely changed among the microbiota groups at 12–16 weeks postexposure to high-LET radiation. For example, *Lactobacillus murinus* was found in RM colons, stayed high in RM post-IR, but yielded even higher in abundance in CM post-IR, if compared to the level prior IR. In RM females, *Turicibacter species* and *Lachnospiraceae bacterium* were elevated by LBJ oral gavage and ^{1}H-IR (Supplementary Table 1), as like *Barnesiella* species have been shown to increase during arthritis resistance (21).

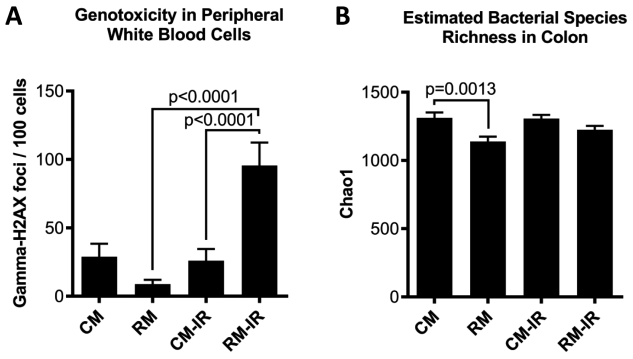

Figure 1. Effects of gut bacteria on radiation-induced systemic genotoxicity. (**A**) Genotoxicity was measured in peripheral blood leukocytes from isogenic C57BL/6J pinked-eyed unstable ($p^{un\ +/+}$) mice harboring either CM or wild-type RM before and after IR. CM-IR ($n = 9$) and RM-IR ($n = 9$) mice were exposed to ^{1}H (1.5 Gy, 2 GeV/n) and the amounts of γ-H2AX foci were assessed in blood lymphocytes at 4 weeks post-IR and compared with sham-irradiated untreated vehicle ($n = 7$ for CM and $n = 8$ for RM) by ANOVA. $P = 0.2383$ for CM vs. RM and $P = 0.8609$ for CM vs. CM-IR, $P < 0.0001$ for CM-IR vs. RM-IR & RM vs. RM-IR. (**B**) Bacterial richness in colon was estimated using Chao1 analyses of gut bacteria in sham CM and RM mice (see graph, $P = 0.0013$) and in both groups as exposed to high-LET radiation. $P = 0.9306$ CM vs. CM-IR and $P = 0.0634$ for RM vs. RM-IR. Error bars indicate SEM.

Anti-genotoxicity effect of CM is induced by neutralization of IL-17

Next, we investigated LBJ interaction with host responses to ionizing radiation in the SI, and its impact on the expression of radiation-protecting gene markers, including fasting-induced adipose factor (Fiaf) (22) and systemic IL-17 (23). The expression of Fiaf in CM blood was chosen as a marker for systemic anti-inflammatory stimuli ($P = 0.00046$; CM < RM) and IFN-γ ($P = 0.039$) was found elevated in RM mice (Supplementary Figure 1A). Regardless of intestinal microbiota compositions, irradiated female CM mice showed a reduction of peripheral IL-17 compared to male mice (Supplementary Figure 1B). In order to initiate anti-genotoxicity effects (Figure 2A and B) and an increase of BIP *Lactobacillus* in post-IR mimicking CM (Table 1), females of both microbiota groups (CM and RM) were intraperitoneally injected neutralizing anti-IL-17 antibodies one day before, 9 h and 2 days after exposure to high-LET silicon ions (1.5 Gy, ^{28}Si, 850 MeV/u). Micronuclei formation in normochromatic erythroblasts in blood was clearly induced by radiation and at higher level in RM than CM mice, supporting the genotoxicity-microbiota linkage for microbiota restriction due to exogenous factors. Anti-IL-17 treatment in both microbiota groups resulted in a significant reduction of micronuclei in blood cells (Figure 2B, $P < 0.0001$ for treatment, IR at the age of 3–4 months). Lower blood protein was measured concerning IL-17 (Figure 2C, $P < 0.008$ Anti-IL-17 vs. Anti-Il-17 and IR in CM), and in the absence of IL-17, TGF-β was significantly downregulated in the antibody treated RM mice up to 3 weeks post-IR (Figure 2D, $P = 0.0160$ for microbiota and $P = 0.0006$ for IR). IL-17 was put back to higher levels of protein in blood in the anti-IL-17 antibody treated mice after 3 weeks, upregulated in the intestine of the vehicle CM mice (Supplementary Figure 2A) and not completely neutralized in the SI in irradiated RM mice. We also found an influence of IR on nuclear factor-kappa B (NF-κB) along with, and in a combination of antibody treatment and IR, with IL-17 gene expression in blood (Supplementary Table 3).

Microbiota restriction augmented bone micro-structure

Bacterial strains identified in RM were associated with a regenerative cell growing effect on normal tissue radiation responses in skeletal bone in RM mice, which was less prominent in the CM phenotype. RM female mice showed improved micro-architectural bone structure compared with CM mice delayed after 6 weeks post-particle radiation exposure (1.5 Gy, ^{28}Si, Figure 3). Female RM mice that were injected neutralizing anti-IL-17 antibody showed significantly improved bone phenotypes, bone density and trabecular bone volume fraction compared to anti-IL-17 modulated CM mice (Figure 3A-C); neutralized RM mice revealed higher trabecular numbers than irradiated and anti-IL-17 treated RM mice ($P = 0.0197$), as well as sham-, and irradiated, CM mice (Figure 3C). Trabecular thickness

Table 1. Categorical analysis (edge R) of gut bacteria in CM and RM mice before and after IR

CM	RM	CM-IR	RM-IR	Genus[a,b]
Colon[c]				
12.2[d]	45.0[d]			[a]Hymenobacteraceae
9.0[d]	0.0[d]	9.6[e]	0.0[e]	*Helicobacter*
23.6[d]	0.0[d]	8.0[e]	0.0[e]	*Helicobacter*
1.6[d]	6.1[d]	2.0[e]	10.3[e]	[a]Hymenobacteraceae
6.7[d]	0.1[d,f]	4.5[e]	1.3[e,f]	*Bacteroides*
2.2[d]	0.6[d,f]		3.4[f]	*Muribaculum*
0.6[d]	0.1[d]	2.2[e]	0.1[e]	*Lactobacillus*
0.0[d]	4.0[d]	0.0[e]	3.0[e]	*Muribaculum*
Small intestine[c]				
5.4[d]	45.6[d]			[a]Hymenobacteraceae
17.6[d]	0.0[d]	2.3[e]	0.0[e]	*Ureaplasma*
0.8[d]	7.2[d]			*Muribaculum*
	0.0[f]	0.0[e]	7.7[e,f]	[a]Hymenobacteraceae

Values in cells are mean relative sequence abundances (%).
[a]Indicates higher level taxa.
[b]Additional taxonomic information and correlation data with DSBs in blood lymphocytes is available in Supplementary Table 2.
[c]For each taxa (row), values with the same letter are different (edgeR analyses, $P < 0.05$, FDR-corrected). Taxa shown are the OTUs that have the 10 highest mean relative abundances. $n = 7$, 8, 9, and 10 for CM, RM, CM-IR, and RM-IR, respectively.
[d]Taxa are compared between CM and RM mice.
[e]Taxa are compared between CM-IR and RM-IR mice.
[f]Taxa are compared between RM and RM-IR mice.

was similar between irradiated mice in both groups (0.0323 and 0.0316 mm mean values for RM-IR and CM-IR, respectively). Tibiae cortical thickness was measured in both microbiota groups before and after IR and determined to be higher in all CM mice.

By comparing tissue-specific multiple target genes under IL-17 neutralization, intestinal microbiota differences and IR were assessed to influence gene expression in the SI (Figure 4A) and the bone marrow (Figure 4C) at 6 weeks post-IR, again. Expression of all measured cytokines in the SI was higher in RM mice relative to CM mice. Particularly the expression of the pro-inflammatory cytokine TNF (non-irradiated mice) as well as the chemokine C–C motif ligand 20 (CCL20) was upregulated in irradiated and sham-irradiated mice (Supplementary Table 3, $P = 0.03377$). Along with harvesting long bones for *ex vivo* micro-structure analysis, the endpoint for measuring signaling markers was set post the acute radiation injury time-point to avoid any necrosis effects. Only the expression of Fiaf was relatively higher in CM mice in SI ($P = 0.03377$).

Together, we also measured the expression of some of these targets in blood and bone marrow (Figure 4B and C). While we observed a significant reduction in NF-κB1 expression in blood ($P = 0.03377$) in IL-17 neutralized RM mice due to IR, any other targets showed significant changes due to microbiota or IR, suggesting that their impact on the investigated targets were less important in blood and bone marrow.

Overall, TNF was highly upregulated in irradiated and non-irradiated bone marrow in CM mice (Figure 4C, $P = 0.056$, and Supplementary Figure 2B), but downregulated in the SI (Figure 4A). Microbiota restriction reduced inflammatory markers of TNF in marrow and chemokine (CCL20) in marrow compared to SI, under anti-IL-17 treatment (Figure 4).

Discussion

Shifts in the gut microbiota in response to ionizing radiation have been briefly described in human radiotherapy patients (24). Whereas gut microbes and probiotics administration were demonstrated to influence the effectiveness of cancer immunotherapy (25,26), our findings with LBJ suggest that caution may be warranted in the selection of probiotic adjuvants in cancer treatment. Male mice younger than 4 months-old were inoculated with LBJ; but the probiotics strain was nor, eradicating *Ureaplasma felinum* in the SI, nor *Helicobacter rodentium* in the colon (Supplementary Table 1). In our study, in the SI in irradiated female CM mice, and in all RM mice when compared with CM mice, bacterial phylotype *Muribaculum intestinale* was more than 10-fold increased and reduced by LBJ and IR. *Lactobacillus animalis* (detected with 100% sequence identity in CM mice, Supplementary Table 2A) was administrated to mice and has been shown to decrease IL-17 (27), a gene which is related to intestinal microbiota. Prior research, in contrast, has been shown that eradicating the carcinogenesis-promoting bacteria *H. pylori* was associated with increased rates of gastroesophageal reflux disease (GERD) and esophageal adenocarcinoma (28).

We addressed the inhibition of high-LET-induced osteoclastogenesis in the anti-inflammatory time-dependent cross-talk between bone marrow cells and intestinal mucosa cells, and therefore applied heavy ion radiation at higher dose (1.5 Gy) than determined to induce persistent bone loss by the oxidative stress response itself (17). We are interested in exploring the mechanistic link related to a reciprocal interplay between IL-17-expressing T helper (h) 17 in SI (29), regulatory T cells and its dependence on TGF-β that would shed light on multiple pathways applying to osteoclastogenesis and IL-17 associated anti-tumor activity (23). Bone resorption in irradiated CM mice is associated with the high expression of TNF in marrow, and the significant over-expression of several target genes (IL-17, TGF-β, and NF-κB) upon radiation treatment. Irradiated female and male CM mice showed a reduction of peripheral IL-17 compared to sham male mice. Anti-apoptotic NF-κB1 sustained upregulated in blood of irradiated female CM mice. Sublethal high-LET and high-charge and energy (HZE) ion exposure of mice was applied to compare gene expression in the blood of sham RM mice with female CM mice (Supplementary Figure 1B). Furthermore, TNF has been investigated to promote

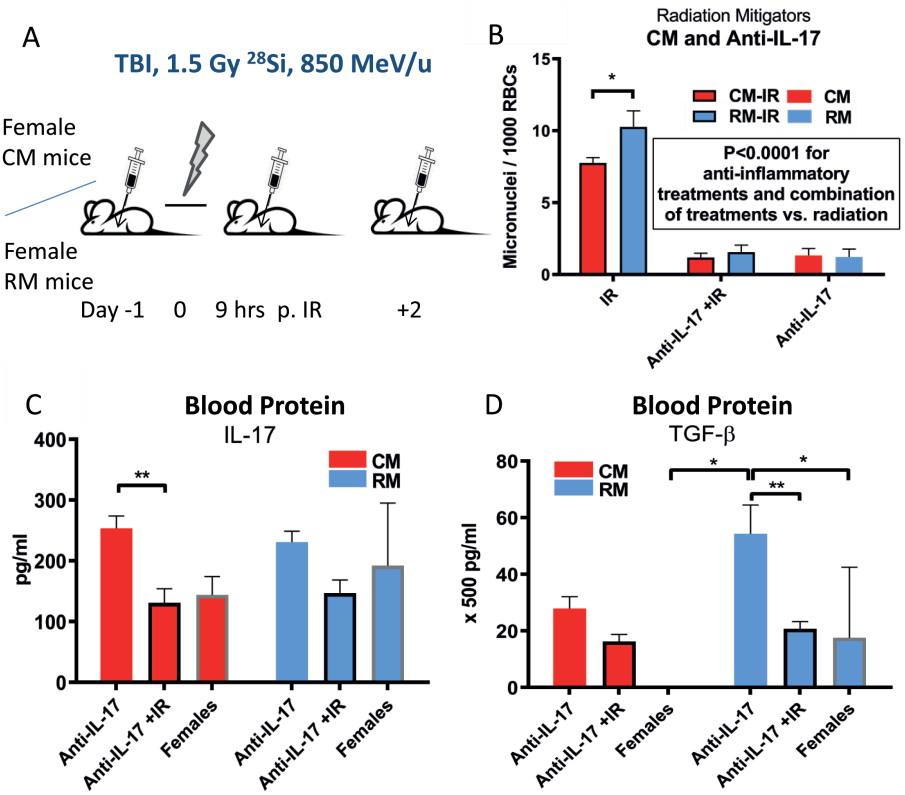

Figure 2. Microbiota-independent IL-17 neutralization in blood alleviates high-LET-induced genomic instability. (**A**) Schematic representation of systemic IL-17 neutralization upon radiation exposure. (**B**) Micronuclei staining showing high-LET-induced genomic instability is alleviated by IL-17 neutralization, as assayed in normochromatic erythroblasts. (i) IR = High-LET irradiation (n = 6 for CM and n = 4 for RM). (ii–iii) Anti-IL-17 treatment = female Ab-treated CM (n = 6) and RM mice (n = 6). Ab-treated and irradiated CM (n = 5) and RM mice (n = 6). Tukey's multiple comparisons test was used in a two-way ANOVA for statistical adjustment. P=0.0476 for CM-IR vs. RM-IR. Error bars indicate SEM. (**C** and **D**) ELISA assessing systemic levels of IL-17 and TGF-β in peripheral blood at 3 weeks post-IR. ANOVA was used for statistical analyses. (*) = $P < 0.05$; (**) = $P < 0.01$; n = 3 and n = 2 for sham-treated female CM and RM mice, respectively).

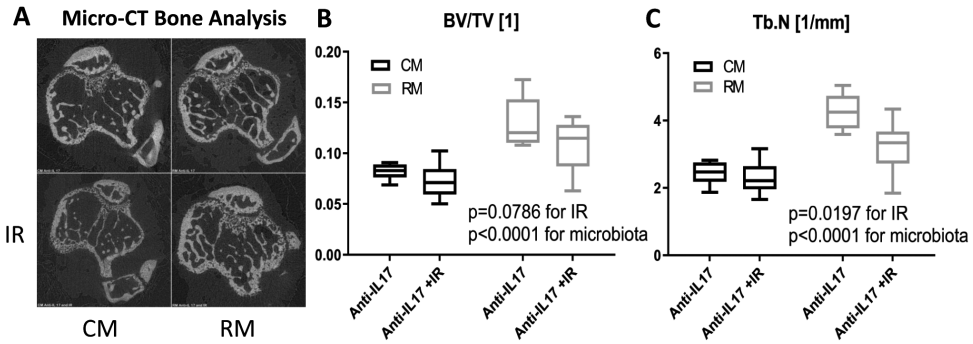

Figure 3. Microbiota restriction augments bone micro-architecture. (**A**) Tibiae analysis by micro-CT at 6 weeks post ^{28}Si irradiation (1.5 Gy; 850 MeV/u). Top left: Anti-IL-17 treated CM mice; top right: Anti-IL-17 treated RM mice; bottom left: Anti-IL-17 treated and irradiated CM mice, and bottom right: Anti-IL-17 treated and irradiated RM mice (n = 6 in all groups). (**B**) Relative bone volume—BV/TV. (**C**) Trabecular numbers—Tb.N. Two-way ANOVA was used for statistical analyses. Mean Tb. thickness and Tb. spacing were 0.0316 and 0.4029 mm (anti-Il-17 CM-IR; n = 6) and 0.0323 and 0.2574 mm (anti-IL-17 RM-IR; n = 6). Mean cortical thickness was 0.1573 mm (anti-IL-17 CM; n = 3), 0.1336 mm (anti-IL-17 CM-IR; n = 4), 0.1422 mm (anti-IL-17 RM; n = 3), and 0.1302 mm (Anti-IL-17 RM-IR; n = 4).

the expression of receptor activator of nuclear factor-κB ligand (RANKL), may drive systemic osteoclastogenesis in CM mice (30), and HZE-induced proliferation in SI in RM mice (12).

In summary, we showed that microbiota restriction reduced inflammatory TNF in marrow and IL-17 in blood. Chemokine CCL20 was reduced in SI compared to marrow in CM mice, but upregulated by IR (P = 0.0965) and in RM (P = 0.03377), while bone micro-structure in tibiae showed any radiation-induced bone loss, thus triggering anti-inflammatory and regenerative signaling cascades (31) mediated by intestinal microbiota (32). Long bones from female RM mice revealed highest improved overall microarchitecture, and tibiae in female RM mice showed higher trabecular numbers at past 6 weeks post-IR than tibiae in female CM mice (Figure 3). IR affected significantly different expression of macrophage-stimulating IL-2 in LBJ-inoculated RM mice (P = 0.0046); a cytokine which is expressed by macrophages and DCs, and like IL-12 may function to inhibit osteoclastogenesis, while it stimulates Th1 cell differentiation

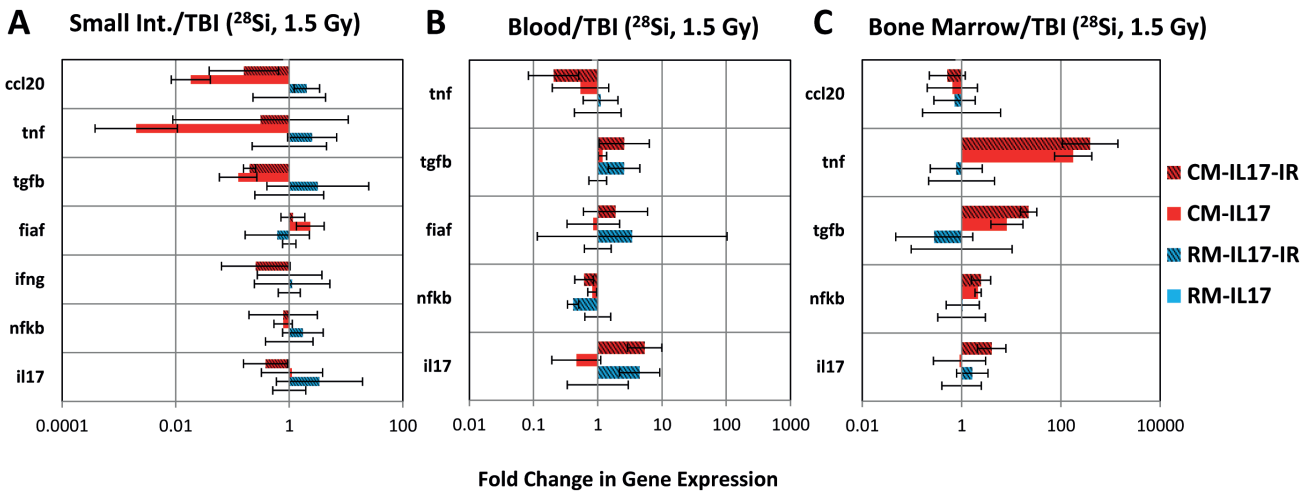

Figure 4. Gene expression in CM and RM mice treated with neutralizing anti-IL-17 antibodies and irradiated in (**A**) SI, (**B**) Peripheral blood, and (**C**) Bone marrow (BM). Female CM ($n = 6$) and RM ($n = 6$) mice at the age of 3 months were intraperitoneally injected with 100 µL anti-IL-17 mAb (20 µg) before, and on day 0 and day 2 after exposure to ^{28}Si (1.5 Gy, 850 MeV/u). CM-IL17-IR = female Ab-treated and irradiated CM mice ($n = 6$), RM-IL17-IR = Ab-treated and irradiated RM mice ($n = 7$). Mann–Whitney *U* test was used to compare the average ΔC_t values of each group.

(31,33) against a protective effector immunity in colorectal cancer (34). The antigen-specific effect of IL-12 when released by dendritic cells (DCs) in conjunction with antitumor cytolytic CD8$^+$ T cells (35,36), is first counteracting to the immune-stimulating function of cytokines, such as IL-17 and IL-1β (23). Secondly, type I IFN is involved in the intratumoral accumulation of DCs (36), but IL-2 has been shown to be higher expressed and upregulated in irradiated and LBJ-inoculated CM mice due to treatment, as measured in peripheral blood (Supplementary Table 3). Specifically, IFN-γ was slightly overexpressed in the SI in sham-treated females compared with males. This finding supported high IFN-γ expression in all CM mice in SI (Supplementary Figure 2A). But IFN-γ has been found relatively downregulated in the SI, when female CM mice were injected neutralizing anti-IL-17 antibodies pre- and post-IR and irradiated (Figure 4A), indicating an intestinal immune-regulatory context with higher radiation susceptibility in females. *Turicibacter* was one of the BIPs found in female colons, and the administration of LBJ suspension changed this phylotype abundance to be greater in RM than CM. By contrast, *Lachnospiraceae* were highest in female RM-IR and correlated with systemic genotoxicity, but were not changed in CM-IR. Therefore, few indicator phylotypes were correlated with the acute repair of radiation-induced genotoxicity. *Helicobacter typhlonius* was found in the colon in both sex groups, and *L.murinus* was found in young male colons; in comparison, pathogenic *U.felinum* species was specifically present in male radiation-resistant SI in CM mice and depleted by IR.

Supplementary material

Supplementary data are available at *Carcinogenesis* online.

Funding

This work was supported by NASA (grant NNX11AB44G to R.H. Schiestl, J. Borneman) and Fulbright Grant for Teaching and Research (I. Maier).

Acknowledgements

The authors acknowledge Dr. Joshua Alwood (NASA AMES Research Center) and Dr. Aya Westbrook (UCLA) for scientific support and discussions, and Christine Ausserhuber for technical assistance. We cordially thank Drs. Adam Rusek and Peter Guida and their teams at NSRL for assistance with the radiation experiment.

Conflict of Interest Statement: None declared.

References

1. Roy, S. *et al.* (2017) Microbiota: a key orchestrator of cancer therapy. *Nat. Rev. Cancer*, 17, 271–285.
2. Toller, I.M. *et al.* (2011) Carcinogenic bacterial pathogen Helicobacter pylori triggers DNA double-strand breaks and a DNA damage response in its host cells. *Proc. Natl. Acad. Sci. U.S.A.*, 108, 14944–14949.
3. Arthur, J.C. *et al.* (2012) Intestinal inflammation targets cancer-inducing activity of the microbiota. *Science*, 338, 120–123.
4. Yamamoto, M.L. *et al.* (2013) Intestinal bacteria modify lymphoma incidence and latency by affecting systemic inflammatory state, oxidative stress, and leukocyte genotoxicity. *Cancer Res.*, 73, 4222–4232.
5. Goto, S. *et al.* (2002) Delayed cell cycle progression in human lymphoblastoid cells after exposure to high-LET radiation correlates with extremely localized DNA damage. *Radiat. Res.*, 158, 678–686.
6. Bourton, E.C. *et al.* (2011) Prolonged expression of the γ-H2AX DNA repair biomarker correlates with excess acute and chronic toxicity from radiotherapy treatment. *Int. J. Cancer*, 129, 2928–2934.
7. Celeste, A. *et al.* (2002) Genomic instability in mice lacking histone H2AX. *Science*, 296, 922–927.
8. Gueulette, J. *et al.* (2001) Proton RBE for early intestinal tolerance in mice after fractionated irradiation. *Radiother. Oncol.*, 61, 177–184.
9. Feng, T. *et al.* (2011) Interleukin-12 converts Foxp3+ regulatory T cells to interferon-γ-producing Foxp3+ T cells that inhibit colitis. *Gastroenterology*, 140, 2031–2043.
10. Neta, R. *et al.* (1994) IL-12 protects bone marrow from and sensitizes intestinal tract to ionizing radiation. *J. Immunol.*, 153, 4230–4237.
11. Alwood, J.S. *et al.* (2015) Ionizing radiation stimulates expression of pro-osteoclastogenic genes in marrow and skeletal tissue. *J. Interferon Cytokine Res.*, 35, 480–487.
12. Maier, I. *et al.* (2014) Intestinal microbiota reduces genotoxic endpoints induced by high-energy protons. *Radiat. Res.*, 181, 45–53.
13. Wardill, H.R. *et al.* (2017) Determining risk of severe gastrointestinal toxicity based on pretreatment gut microbial community in patients receiving cancer treatment: a new predictive strategy in the quest for personalized cancer medicine. *Curr. Opin. Support. Palliat. Care*, 11, 125–132.
14. Jacobs, J.P. *et al.* (2016) A disease-associated microbial and metabolomics state in relatives of pediatric inflammatory bowel disease patients. *Cell. Mol. Gastroenterol. Hepatol.*, 2, 750–766.

15. Fujiwara, D. *et al.* (2008) Systemic control of plasmacytoid dendritic cells by CD8+ T cells and commensal microbiota. *J. Immunol.*, 180, 5843–5852.
16. Bouxsein, M.L. *et al.* (2010) Guidelines for assessment of bone microstructure in rodents using micro-computed tomography. *J. Bone Miner. Res.*, 25, 1468–1486.
17. Bandstra, E.R. *et al.* (2008) Long-term dose response of trabecular bone in mice to proton radiation. *Radiat. Res.*, 169, 607–614.
18. Van der Heijden, P.J. *et al.* (1987) Improved procedure for the isolation of functionally active lymphoid cells from the murine intestine. *J. Immunol. Methods*, 103, 161–167.
19. Ruegger, P.M. *et al.* (2014) Improved resolution of bacteria by high throughput sequence analysis of the rRNA internal transcribed spacer. *J. Microbiol. Methods*, 105, 82–87.
20. Ge, Z. *et al.* (2017) Helicobacter hepaticus cytolethal distending toxin promotes intestinal carcinogenesis in 129Rag2-deficient mice. *Cell Microbiol*, 19:e12728.
21. Gomez, A. *et al.* (2012) Loss of sex and age driven differences in the gut microbiome characterize arthritis-susceptible 0401 mice but not arthritis-resistant 0402 mice. *PLoS One*, 7, e36095.
22. Crawford, P.A. *et al.* (2005) Microbial regulation of intestinal radiosensitivity. *Proc. Natl. Acad. Sci. U.S.A.*, 102, 13254–13259.
23. Hemdan, N.Y. *et al.* (2012) Key molecules in the differentiation and commitment program of T helper 17 (Th17) cells up-to-date. *Immunol. Lett.*, 148, 97–109.
24. Nam, Y.D. *et al.* (2013) Impact of pelvic radiotherapy on gut microbiota of gynecological cancer patients revealed by massive pyrosequencing. *PLoS One*, 8, e82659.
25. Vétizou, M. *et al.* (2015) Anticancer immunotherapy by CTLA-4 blockade relies on the gut microbiota. *Science*, 350, 1079–1084.
26. Sivan, A. *et al.* (2015) Commensal Bifidobacterium promotes antitumor immunity and facilitates anti-PD-L1 efficacy. *Science*, 350, 1084–1089.
27. Karunasena, E. *et al.* (2013) Effects of the probiotic Lactobacillus animalis in murine Mycobacterium avium subspecies paratuberculosis infection. *BMC Microbiol.*, 13, 8.
28. Talebi Bezmin Abadi, A. *et al.* (2014) Helicobacter pylori: a beneficial gastric pathogen? *Front. Med. (Lausanne)*, 25.
29. Esplugues, E. *et al.* (2011) Control of TH17 cells occurs in the small intestine. *Nature*, 475, 514–518.
30. Kearns, A.E. *et al.* (2008) Receptor activator of nuclear factor kappaB ligand and osteoprotegerin regulation of bone remodeling in health and disease. *Endocr. Rev.*, 29, 155–192.
31. Ciucci, T. *et al.* (2015) Bone marrow Th17 TNFα cells induce osteoclast differentiation, and link bone destruction to IBD. *Gut*, 64, 1072–1081.
32. Maier, I. *et al.* (2015) Evidence from animal models: is a restricted or conventional intestinal microbiota composition predisposing to risk for High-LET radiation injury? *Radiat. Res.*, 183, 589–593.
33. Sato, K. *et al.* (2006) Th17 functions as an osteoclastogenic helper T cell subset that links T cell activation and bone destruction. *J. Exp. Med.*, 203, 2673–2682.
34. Bhattacharya, N. *et al.* (2016) Normalizing microbiota-induced retinoic acid deficiency stimulates protective CD8(+) T cell-mediated immunity in colorectal Cancer. *Immunity*, 45, 641–655.
35. Presley, L.L. *et al.* (2010) Bacteria associated with immunoregulatory cells in mice. *Appl. Environ. Microbiol.*, 76, 936–941.
36. Fuertes, M.B. *et al.* (2011) Host type I IFN signals are required for antitumor CD8+ T cell responses through CD8{alpha}+ dendritic cells. *J. Exp. Med.*, 208, 2005–2016.